Oecologia (2011) 166:357–368
DOI 10.1007/s00442-010-1867-y

POPULATION ECOLOGY - ORIGINAL PAPER

Modelling the effect of directional spatial ecological processes at different scales

F. Guillaume Blanchet · Pierre Legendre · Roxane Maranger · Dominique Monti · Pierre Pepin

Received: 22 June 2009 / Accepted: 22 November 2010 / Published online: 19 December 2010

Abstract During the last 20 years, ecologists discovered the importance of including spatial relationships in models of species distributions. Among the latest developments in modelling how species are spatially structured are eigenfunction-based spatial filtering methods such as Moran's eigenvector maps (MEM) and principal coordinates of neighbour matrices (PCNM). Although these methods are very powerful and flexible, they are only suited to study distributions resulting from non-directional spatial processes. The asymmetric eigenvector map (AEM) framework, a new eigenfunction-based spatial filtering method, fills this theoretical gap. AEM was specifically designed to model spatial structures hypothesized to be produced by directional spatial processes. Water currents, prevailing wind on mountainsides, river networks, and glaciations at historical time scales are some of the situations where AEM can be used. This paper presents three applications of the method illustrating different combinations of: sampling schemes (regular and irregular), data types (univariate and multivariate), and spatial scales (metres, kilometres, and hundreds of kilometres). The applications include the distribution of a crustacean (*Atya*) in a river, bacterial production in a lake, and the distribution of the copepodite stages of a crustacean on the Atlantic oceanic shelf. In each application, a comparison is made between AEM, MEM, and PCNM. No environmental components were included in the comparisons. AEM was a strong predictor in all cases, explaining 59.8% for *Atya* distribution, 51.4% of the bacterial production variation, and 38.4% for the copepodite distributions. AEM outperformed MEM and PCNM in these applications, offering a powerful and more appropriate tool for spatial modelling of species distributions under directional forcing and leading to a better understanding of the processes at work in these systems.

Keywords Asymmetric eigenvector maps (AEM) · *Atyidae* · Bacterial production · *Calanus finmarchicus* · Current · Directional spatial process · Flux · Lake St. Pierre · Moran's eigenvector maps (MEM)

Communicated by Craig Osenberg.

Electronic supplementary material The online version of this article (doi:10.1007/s00442-010-1867-y) contains supplementary material, which is available to authorized users.

F. G. Blanchet · P. Legendre · R. Maranger
Département de Sciences Biologiques, Université de Montréal, Succursale Centre-ville, C.P. 6128, Montréal, QC H3C 3J7, Canada

D. Monti
EA-926 DYNECAR, Laboratoire de Biologie Marine, Université des Antilles et de la Guyane, Campus de Fouillole, BP 592, 97157 Pointe-à-Pitre Cedex, Guadeloupe, French West Indies

P. Pepin
Department of Fisheries and Oceans, P.O. Box 5667, St John's, NL A1C 5X1, Canada

Present Address:
F. G. Blanchet (✉)
Department of Renewable Resources, University of Alberta, 751 General Service Building, Edmonton, AL T6G 2H1, Canada
e-mail: gblanche@ualberta.ca

Introduction

The importance of spatial structures for the interpretation of ecological data is now widely recognized (Legendre and Fortin 1989; Legendre 1993; Peterson and Parker 1998; Legendre and Legendre 1998; Fortin and Dale 2005). Indeed, environmental forcings of many kinds, which have spatial components, affect the spatial distributions of species in

ecosystems. This idea has long been understood by ecologists; it forms the classical environmental control model which is based on ecological niche theory (Hutchinson 1957). In this paper, we focus on directional physical processes hypothesized to influence species distributions, either directly by transporting organisms or indirectly by transporting particles, nutrients, and other elements on which the organisms depend.

For example, dominant winds or currents generate directional gradients by advecting motile organisms and affecting the physical conditions of sessile organisms. Other directional patterns are found in river networks where water is flowing downstream, carrying chemicals, particles and planktonic organisms, whereas nektonic organisms may be migrating against the prevailing current.

Some recently developed methods of analysis incorporate the spatial relationships into models of the response data. In particular, methods developed by geostatisticians consider both the spatial structures and the physical gradients (Cressie et al. 2006; ver Hoef et al. 2006; Peterson et al. 2007; Peterson and ver Hoef 2010; ver Hoef and Peterson 2010). These methods seem suitable and well adapted to analyse whole networks of streams or rivers; however, geostatistical approaches may not produce strong predictive models when only small sections of streams are sampled, which is often the case in ecological studies.

The development of the principal coordinates of neighbour matrices (PCNM; Borcard and Legendre 2002; Borcard et al. 2004) and its generalization, the Moran's eigenvector maps (MEM; Dray et al. 2006) framework, provided powerful tools to study the spatial structures of individual species and communities at multiple scales and in greater detail. These methods could be applied to directional spatial processes found in streams and rivers or along ocean currents, but their failure to consider the directional nature of these processes is a shortcoming. In these methods, the influence of broad-scale gradients must be removed (the data must be detrended) prior to analysis, thereby excluding that portion of the spatial structure (the gradient information) from the analysis. To solve this problem, Blanchet et al. (2008b) proposed the asymmetric eigenvector maps (AEM) method, an eigen-based spatial filtering method (Griffith and Peres-Neto 2006) which differs from the MEM framework.

When performing a spatial analysis using eigenfunctions, the sampled site coordinates or the connexions among the sites are decomposed into a number of spatial variables (eigenvector maps, or eigenfunctions). A detailed explanation of how eigenvector maps are constructed is presented by Dray et al. (2006) for the MEM framework and by Blanchet et al. (2008b) for the AEM framework. After their construction, the resulting spatial variables are used in linear models [multiple regression for univariate, canonical redundancy analysis (RDA) for multivariate response data] like any other explanatory variable to model a response variable or data table. These two frameworks generate a large number of explanatory variables, often one variable less than the number of sites. It is thus important to choose the best variable(s) to model the response with an appropriate variable selection procedure such as the one proposed by Blanchet et al. (2008a).

The strength of spatial eigenfunctions is that they can be used to analyse either univariate or multivariate response data. They are also orthonormal, each spatial variable being perpendicular to the others. This is a convenient property because it ensures that there is no collinearity among the spatial eigenfunctions.

The weakness of spatial eigenfunction analysis is the difficulty of interpreting each variable independently. Various strategies have been tried to overcome that problem; the most commonly used are presented in Borcard et al. (2004).

In the present paper, our objective is to illustrate the application of AEM analysis to real ecological data using three illustrative datasets which come from different types of ecosystems (stream, fluvial lake, and ocean) and represent different spatial scales (metres, kilometres, and hundreds of kilometres), contrasting sampling designs (regular and irregular two-dimensional surfaces), and univariate or multivariate data. The three datasets have in common that directional water currents influence the response data, which generates a spatial asymmetry in the response. To show the efficiency of AEM analysis, the results will be compared to analyses carried out using the MEM and PCNM frameworks. The stream illustration assesses the spatial distribution of the crustacean *Atya innocous* in a reach of Capesterre River, Guadeloupe. The fluvial lake example is a study of bacterial production in Lake St. Pierre, Québec, Canada. The ocean example models the distribution of the copepodite stages of the crustacean *Calanus finmarchicus* along the eastern shores of Newfoundland and Labrador. These examples offer the opportunity to give extra practical details about the application of the AEM method.

The goal of this paper is to compare spatial modelling methods in different ecological situations and measure the importance of directional spatial processes in each system. The correct identification of directional processes will refine our understanding of the ecological processes at work in the ecosystems. Environmental variables were not included in the analyses in order to place the emphasis on the spatial components, either directional or isometric.

Basic theory of the AEM method

A detailed account of the construction of AEM is found in Blanchet et al. (2008b). The steps are summarized in Table A1 and Fig. A1 (Electronic Appendix A). AEM variables are spatial eigenvectors, in the same way as MEMs. Their

construction involves a connexion diagram among sampling sites, the connexions being directional in AEM, which is not the case in MEM or PCNM. As in MEM, the links can receive weights representing the ease of communication of matter or information among the sites; the links in AEM can be based, for example, on geographic distances, flow models, or current speed. AEMs can be used in models in the same way as researchers use variables from the MEM or PCNM frameworks.

When constructing AEMs, there are very often $n - 1$ variables created, n being the number of sites. This situation makes it impossible to test the significance of a regression model that uses all AEM variables because of the lack of degrees of freedom. A part of the AEMs model positive spatial correlation while the remaining AEMs model negative spatial correlation. In some studies, it is clear that only the AEMs modelling positive spatial correlation are of interest and should be used. For studies where the exclusive use of AEMs modelling positive spatial correlation is not clear, Blanchet et al. (2008a) described a procedure which will be used in the ecological illustrations herein, where MEMs and AEMs are used and compared. The approach consists in separating the set of spatial variables in two portions, one modelling positive spatial correlation and the other negative spatial correlation. The two groups of MEM or AEM variables are then considered as potential explanatory variables in the analysis. The two groups are tested separately for significance and the results of the two tests are combined.

Associated with each AEM eigenfunction is an eigenvalue. In contrast to the MEM framework, all AEM eigenvalues are positive, owing to their method of construction (Blanchet et al. 2008b). AEM eigenvalues are not direct measures of spatial correlation, as is the case for MEM eigenvalues which are perfectly correlated to Moran's I. The response variables need not be detrended when using AEM, contrary to PCNM and MEM eigenfunctions: the trend is an important component of directional spatial patterns, so it must be kept in the data to allow it to be brought out by the AEM analysis. In contrast, a significant spatial trend can influence the selection of PCNM and MEM variables by forcing the selection of particular eigenfunctions (in the case of regular grids, the eigenfunctions with odd ranks model gradients). With AEM, the direction of the flow, which is often correlated with the trend, is known a priori and is considered in the construction of the directional spatial variables.

Illustrations using real ecological data

Method of analysis

Although the three illustrative datasets described in the next sections are very different from one another, we are going to apply the same analytical procedure when comparing the results of the different spatial modelling methods. This offers the dual advantage of showing how each method behaves in an asymmetric directional context and of rendering the three illustrations comparable.

In the three ecological illustrations, the set of eigenfunctions was used to model the response variable(s) as follows. First, a global test using all spatial variables of the considered kind was computed. Because the MEM and AEM frameworks generate too many spatial variables, the set of eigenfunctions was divided in two on the basis of their spatial correlation (positive and negative), as described in the previous section. A detailed explanation of how to split the AEM eigenfunctions in two groups is presented in the paragraph explaining the construction of AEM (three paragraphs down). In all examples, there was no prior information about the expected sign of the spatial correlation; both sets were thus tested and a Šidák correction (Šidák 1967) was applied to assess the global significance of the two sets of variables. The P values after correction will be written P_{corr} to differentiate them from P, a P value calculated prior to correction. If the model was significant at the 5% level, a forward selection procedure was applied, using two stopping criteria as proposed by Blanchet et al. (2008a), to obtain a parsimonious model. Forward selection kept choosing variables until either a given significance level (5% was used in our analyses) was reached or the adjusted coefficient of multiple determination (R^2_{a}; see Eq. 1) of the reduced model reached the value for the full model containing all variables.

A single set of PCNM variables was constructed for each ecological example. The truncation distance was the smallest distance that kept all the sites linked together, except for the Capesterre River example where we used $\sqrt{2}$ as the truncation distance (the length of the diagonal in a regular, square, unit grid).

For each illustration, the connexion diagram used to construct spatial variables through the MEM framework reflected the knowledge we had of the study area; it is thus considered optimal and will not be subject to change. The different sets of spatial variables constructed diverged only by the weights given to the links. For all examples, one set was constructed with equal weights for all links. For the first and second illustrations, weights were functions of the distance. Weights were computed by applying two functions from Dray et al. (2006) to the lengths of the links: $f_1(d_{ij}) = 1 - (d_{ij}/\max(d_{ij}))^{\alpha}$ and $f_2(d_{ij}) = 1/d_{ij}^{\alpha}$. Exponents $\alpha = 1$ and $\alpha = 2$ were considered for each function. f_1 is a concave-down function whereas f_2 is concave-up. The function and exponent combination that produced the best explanation (highest R^2_{a}) was selected (Tables B1 and C1,

Appendices B, C). In the third illustration (*C. finmarchicus* data), along-shelf geostrophic current speed was used instead of distance to weight the edges linking the sites. The mean current speed calculated between two linked sites was used to weight each edge of the connexion diagram. After calculation of the weights, some of them had negative values; these values were replaced by 0. Because a higher current speed means a stronger connexion between the sites, a different weighting function was used for this example: $f_3(d_{ij}) = (d_{ij}/\max(d_{ij}))^{\beta}$. β was set at 0.5 (concave-up), 1 (linear), or 2 (concave-down); the value of β that produced the best explanation (highest R^2_a) was selected (Tables D1, Appendix D).

The connexion diagrams used to construct eigenfunctions in the AEM framework were the same as in MEM. The optimal combinations of function and exponent were recomputed for each AEM application (Tables B1, C1 and D1, Appendices B, C and D). To divide the spatial variables into positively and negatively correlated sets, Moran's I were calculated for each eigenfunction following Gittleman and Kot (1990). This procedure allows the use of an asymmetric distance matrix in the calculation of the Moran's I coefficients. The distance matrix used in this calculation was constructed from the weighted links of the connexion diagram; Fig. A2 (Appendix A) describes the procedure in detail. If the observed value was higher than the expected I value under the hypothesis of absence of spatial correlation, the eigenfunction was considered to model positive spatial correlation; otherwise it was considered to be negatively autocorrelated.

Comparisons among modelling methods was done through variation partitioning (Borcard et al. 1992). The fractions of variation were measured by adjusted R squares (R^2_a). The equation to calculate R^2_a is (Ezekiel 1930; Zar 1999, Eq. 20.23):

$$R^2_a = 1 - \frac{n-1}{n-m-1}(1-R^2). \quad (1)$$

where n is the sample size and m the number of explanatory variables. R^2 is the coefficient of multiple determination, computed as the sum of squares explained by the model divided by the total sum of squares. Ohtani (2000) has shown that R^2_a is an unbiased estimator of the contribution of a set of explanatory variables $\mathbf{X}$ to the explanation of $\mathbf{y}$. Peres-Neto et al. (2006) have shown that R^2_a also has that property in canonical analysis. Each independent fraction (called [a], [b], and [c] in this paper) was tested with 1,000 permutations; the P value is given. The significance level used was 0.05.

For all ecological examples, the PCNM and MEM analyses were carried out on detrended response variables if a linear trend in the direction of the hypothesized spatial process was significant at the 5% level (Borcard and Legendre 2002). In the ocean illustration, because the response data are multivariate, the trend was removed from each response variable (copepodite stage) separately after verifying that a linear model constructed by RDA with all copepodite stages as the response and the geographic coordinates as the explanatory data was significant. AEM analysis was always conducted on non-detrended data. Because of this divergence, we carried out variation partitioning analysis using the non-detrended data as response variable(s), and added the linear trend as a supplemental explanatory variable in the variation partitioning analysis when it was significant.

River (regular grid): spatial microdistribution of a crustacean in Capesterre River (Guadeloupe)

The microdistribution of a crustacean species, *A. innocous* (*Atyidae*), was studied in a mountain reach of Rivière Capesterre (16°4′3″N, 61°35′40″W) on Basse-Terre, the volcanic portion of Guadeloupe, French West Indies. Because one must work on foot in the river, the study was carried out during the dry season when current velocity was moderate. The river reach was sampled in 94 contiguous quadrats of 3 × 3 m forming a regular grid, spatially referenced on a map. Beginning downstream, electric fishing was done using a portable electrofishing device (DEKA Gerätebau, Marsberg, Germany). The low water conductivity in this type of tropical river allowed precise application of electrofishing with limited spatial influence of the anode. The initial purpose of this study was to estimate the links between the presence of *Atya* and physical microhabitat variables. Small buckets were positioned at each site to allow the crustaceans to be released after counting.

We did not find any transformation capable of normalizing the distribution of the response variable. The only significant trend ($P < 0.001$) in the abundance data was perpendicular to the direction of flow. Because there was no significant trend in the direction of flow ($P = 0.361$), the data were not detrended. The 53 PCNMs together explained 47.6% (R^2_a) of the abundances of *A. innocous* ($P < 0.001$). After forward selection, the six selected PCNMs explained 46.2% of the variation of the *Atya* data.

The construction of spatial variables using the MEM and AEM frameworks was based on the connexion diagram presented in Fig. 1a. The best set of variables created through the MEM framework (using function f_2, $\alpha = 1$) gave a global R^2_a of 52.7% of the *Atya* data ($P_{corr} = 0.002$) and were positively autocorrelated. When the forward selection procedure was applied, six MEMs were selected (#1, 12, 13, 16, 25, and 34, presented in Fig. B2, Appendix B); they explained 50.4% of the variation (R^2_a) of the data ($P < 0.001$). The fitted values of the *Atya* model created with the six selected MEM variables are shown in Fig. 1d.

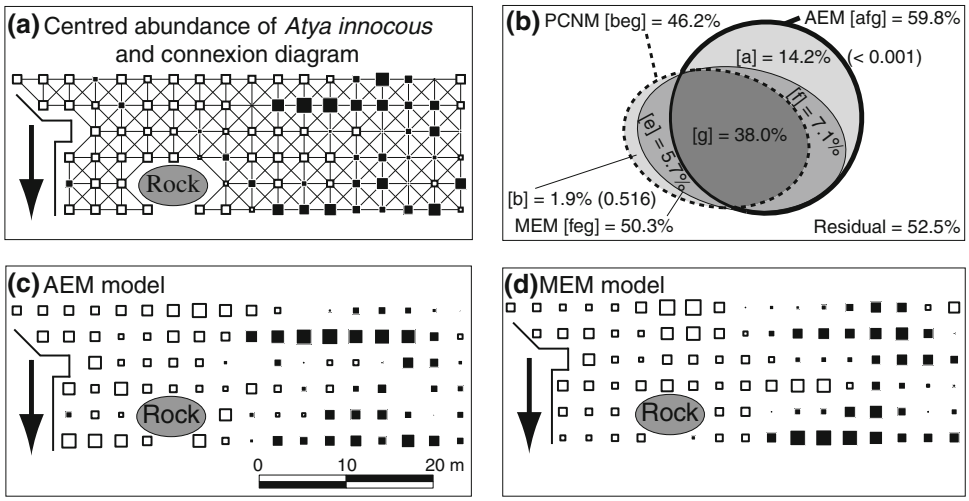

Fig. 1 Spatial modelling of *Atya innocous* distribution in Capesterre River, Guadeloupe. **a** Site locations and connexion diagram used to generate the AEMs and MEMs where the arrow shows the river flow direction, square bubbles represent centred data (black are positive values, white are negative, and size of squares is related to the associated value), sites are spaced by 3 m. Figure A3 (Appendix A) shows how edges linking sites perpendicular to the current were used to build AEMs. The arrow shows the river flow direction. **b** Variation partitioning results between the selected AEMs, MEMs, PCNMs illustrated by a Venn diagram. Fraction sizes are approximations. Letters in brackets correspond to individual fractions of explained variation; values are R^2_a. Values in parentheses represent the *P* values of independent fractions. **c** Fitted values of the selected AEMs. **d** Fitted values of the selected MEMs. The fitted values of the selected PCNMs are not presented because they are very similar to (**d**)

The fitted values of the PCNM model (not shown) are very similar.

For variables from the AEM framework, the best model (using function f_2, $\alpha = 1$) gave a global R^2_a of 60.3% ($P_{corr} = 0.002$) and was positively autocorrelated. This model offers a better depiction of *Atya* distribution than PCNMs and MEM do, with $R^2_a = 47.6$ and 52.7%, respectively (Table B1, Appendix B). Twelve AEM variables were selected by forward selection (#1, 2, 4, 9, 10, 11, 25, 31, 33, 35, 42, and 43 presented in Fig. B1, Appendix B). This reduced the model R^2_a to 59.8% of the variation of the *Atya* data. The fitted values of this model are shown in Fig. 1c. Variation partitioning shows that the AEM model explains the true spatial variation of *Atya* far better than the MEM and PCNM models (Fig. 1b) The variation of the undetrended data explained by the AEM model above and beyond that explained by MEMs and PCNMs is 14.2% ($P < 0.001$). In comparison, the fraction explained exclusively by the MEM model, above and beyond that explained by the AEM model, is 5.3% ($P = 0.010$), and the fraction explained exclusively by the PCNM model, above and beyond that explained by the AEM model, is 7.6% ($P = 0.003$). Detailed results for the other weighting functions considered are presented in Table B1 (Appendix B).

The *Atyidae* prawn family is composed of widespread tropical and temperate crustaceans living mainly in running freshwaters. Most atyids have strong anatomic originalities that determine their food uptake. Those belonging to genus *Atya* are very specialized: instead of using claws like the other Caribbean crustaceans, these animals have the first two pereiopods ending with a big brush made of long bristles. These bristles open like umbrellas in high velocity waters, collecting suspended matter. This species is unique among the *Malacostraca* in having representatives that filter passively by means of the chelipeds (Fryer 1977). Among the three statistical methods compared in this paper, an oriented flow directional method like AEM extracts a significant part of the variation of the *Atya* spatial distribution ($R^2_a = 59.8\%$), greater than the MEM and PCNM methods do (50.4 and 46.2% respectively). Three original characteristics of *Atya* biology are particularly well described by the AEM model: (1) the *Atya* distribution is determined by water flow; the effect of the strictly directional component (water flow direction) can be evaluated as the [a] fraction in Fig. 1b; it represents here 14.2% of the variation of *Atya*; (2) the *Atya* distribution depends on the size of stream pools (Pyron et al. 1999), which, in fast flowing Caribbean rivers, are mainly located along one of the river banks, where the main flow occurs. This generates a non-even distribution of *Atya* individuals between the river banks. In a separate analysis, this lateral trend was estimated to represent 25.8% of the total variation; and (3) *Atya* is gregarious and individuals do not have distinct territories as found in other tropical crustaceans, Palaemonidae for example. The result is a clumped distribution of *Atya* in the river with strong variations of abundances at very fine spatial scale. The third significant fraction of variation detected by AEM, the fraction [f + g] shared with MEM, explains 45.0% of the total variation; it

represents non-oriented spatial processes like aggregations of *Atya* individuals. Figure 1c shows the ability of the AEM model to predict null abundances in the vicinity of high densities of organisms and strong differences at very small scale. Because of its ability to combine longitudinal and lateral orientated processes, the AEM model may be considered as having greater sensitivity than the MEM model for restitution of an aggregative species distribution. These results are very consistent with *Atya* ecology and make this method very attractive for detecting the effects of directional processes on species distributions. This could be of primary importance in river ecology where strong flow directional processes can and do occur.

Fluvial Lake: bacterial production in Lake St. Pierre (Québec, Canada)

Lake St. Pierre (LSP) is a 300-km^2 widening of the St. Lawrence River (46°11′N, 72°50′W), located about mid-way between Montréal and Québec City, QC, Canada. This fluvial lake has an average depth of 3 m. Water is relatively slow flowing (<0.5 m s^{-1}) with the exception of the deep shipping channel which bisects the lake (12 m depth, water velocity >0.5 m s^{-1}). The lake has several juxtaposed and chemically distinct water masses that mix very little laterally (Frenette et al. 2006). The main water masses are: (1) North, draining the nutrient rich, brown soft waters of the Ottawa River; (2) Central, the relatively low dissolved organic carbon (DOC), clear waters of the Great Lakes that funnel through the main shipping channel; and (3) South, from three relatively turbid and nutrient-rich tributaries heavily impacted by agriculture (Vis et al. 2007). The southern mass is more heterogeneous than presented here, but for the present study, only the three main water masses are considered: North, Central, and South. Although the dominant form of organic C available to bacteria is of allochthonous origin, local carbon production by extensive macrophyte communities may be important in the shallow North and South masses.

Heterotrophic bacterial carbon production (BP) is a function of many controlling factors, nutrient availability and carbon lability being predominant. In flowing systems, nutrients can be altered by upstream processing (Newbold et al. 1982), influencing BP rates downstream (Maranger et al. 2005). In the case of a fluvial but heavily vegetated system such as Lake St. Pierre, local production of more labile substrates will influence the relative carbon quality available to the microbes not only at that site but also at sites further downstream (Wetzel 1992). Benthic exchange will also be important given the shallow nature of the system (Hopkinson et al. 1998). The original objective of this study was to look at the spatial heterogeneity of the bacterial production among the water masses. Sampling

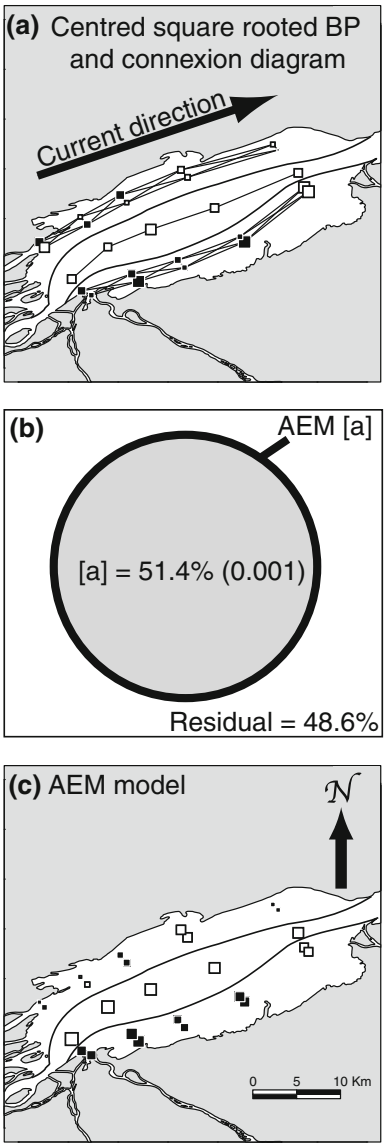

Fig. 2 Spatial modelling of bacterial production (BP) in Lake St. Pierre (white area of maps in **a** and **c**). **a** Site locations and connexion diagram used to generate the AEM eigenfunctions considering that current direction was used to generate AEMs. Square bubbles represent centred square-root transformed data (black are positive values, white are negative, size of squares is related to the associated value). Figure A3 (Appendix A) shows how edges linking sites within each water mass were used to build AEMs. **b** Venn diagram presenting the variation explained by the selected AEMs. Fraction sizes are approximations. The letter in brackets, [a], represents the fraction of explained variation; the value is the R^2_a. The value in parentheses is the associated *P* value. **c** Fitted values of the selected AEM eigenfunctions. Limits of the water masses shown in (**a**) and (**c**) are approximate

was carried out bimonthly in the summer of 2005 and covered the entire lake in a grid pattern of five longitudinal lines and five transects along the axis of flow (Fig. 2a). For this analysis, the sampling units obtained on 18 August 2005 were used. Bacterial production was measured by

radioactive leucine incorporation using the micro-tube centrifugation technique (Smith and Azam 1992). AEM eigenfunction modelling is perfectly suited for this study given the directionality of carbon processing of the bacterial community along the flow axis, the spatial heterogeneity of the system, and the sampling design. Sampling units for nutrient and DOC were obtained at the exact same time; methods for analysis are described elsewhere (Blanchet et al. in press).

When we compared the amount of variation in bacterial production explained using the spatial variables generated from different modelling approaches (PCNM, MEM, and AEM), the most significant set of spatial predictors was the spatially directed AEM (Table C1, Appendix C). For AEM modelling, f_1 with $\alpha = 1$ yielded the best results. The full set of positively autocorrelated variables explained 54.0% (R^2_a) of the variation in bacterial production. A parsimonious and highly significant model was created with 4 AEMs (# 1, 2, 4, and 10, presented in Fig. C1, Appendix C) chosen by forward selection ($R^2_a = 51.4\%$; Fig. 2c), whereas the multidirectional MEMs, built with f_2 and $\alpha = 2$, explained a slightly smaller amount of variation ($R^2_a = 49.4\%$), but was statistically not significant ($P_{corr} = 0.071$). The PCNM model was not significant for this example ($P = 0.763$). Detailed results for the other weighting functions considered are presented in Table C1.

None of the measured environmental variables were able to predict BP as well as the directional spatial AEM descriptors. Bacterial production (μgC L^{-1} h^{-1}) was not related to the various nitrogen forms in the system, which were spatially highly variable (nitrate range: 0–157 μg L^{-1}, total nitrogen range: 293–563 μg L^{-1}), although there was a slight negative tendency with nitrate. BP was weakly related to total phosphorus (TP) explaining only 17.8% of the variation (R^2_a) despite the wide range in concentrations (15–56 μg L^{-1}). There was a slightly stronger significant relationship between BP and DOC with an $R^2_a = 25.4\%$. However, AEM modelling clearly shows the importance of water flow in explaining the spatial variation of bacterial production in Lake St. Pierre.

We expected flow direction to influence the variation in bacterial production, but the fact that the selected eigenfunctions created from directional spatial connectivity alone explained 51.4% of the observed among-site variation was a surprise. The strong differences in source water among the water masses combined with the relatedness of the active bacterial communities from upstream to downstream is one possible reason why the directional spatial model explains so much of the variation among sampling sites. Compared to the other masses, the Central water flows more rapidly and likely resulted in similar substrate availability and bacterial community composition resulting in relatively homogeneous heterotrophic BP from upstream to downstream. This relatedness in the composition of the communities has been observed elsewhere (Masin et al. 2003).

There was considerably less variation in nutrient and DOC concentrations in the Central than in the other water masses, which explains the relative homogeneity in both the measured and AEM model of BP rates (Fig. 2a, c). The overall higher rates and relative decrease in the observed and modelled rates of BP are likely to be a function of the changing abiotic conditions in space, which influenced BP. The waters entering the North and South masses are richer in nutrients; however, the widening of the river reduces the flow of these water masses, increasing algal uptake rates, which results in a greater potential source of labile carbon for bacteria and greater benthic exchange for essential nutrients such as nitrogen and phosphorus. Consequently, nutrients are depleted along the axis of flow if there are no external inputs ultimately impinging on C quality and bacterial productivity. This explains the measured and modelled patterns observed here.

Dissolved organic carbon is the main source of C used by bacteria in aquatic systems, and much of the DOC in large rivers is of allochthonous terrestrial origin coming in from the watershed (Cole and Caraco 2001). Rivers are considered to be reactors as they sequester a considerable amount of C along their flow path (Cole et al. 2007). Interestingly, despite the high macrophyte biomass and primary productivity in LSP (Vis et al. 2007), if we consider the average DOC concentrations of the water masses and their flow rates, we estimate that over 90% of the organic carbon in LSP is allochthonous. However, as the nutrients are consumed along the flow path by primary producers, labile organic carbon (OC) substrates are released and this C is thought to be rapidly sequestered by microbes whereas the recalcitrant allochthonous inputs are thought to be exported (del Giorgio and Pace 2008). Furthermore, terrestrial OC is typically low in nutrients and microbes must depend on dissolved inorganic nutrients to sustain their growth (Caraco et al. 1998). AEM may be particularly useful in predicting PB in large river reaches where no major tributaries are feeding into the section of interest, such as in this example in LSP. AEM analysis of patchier flowing systems, with great variability in localized C and nutrient inputs (Rees et al. 2005), may not work so well for rate processing estimates such as BP, but the method is still applicable to the distribution of species, as illustrated below. However, the strength of the use of AEM directional spatial variables in predicting bacterial production in LSP is that these terms fully integrate the complex interactions between the locally produced labile organic substrates, the nutrients they rely on, and their transformations along the flow path. This integration of complex processing represented in the AEM variables at

least for the spatial analysis of bacterial production in LSP proved to be more effective then classical environmental variables measured at the local sites.

Calanus finmarchicus on the Newfoundland and Labrador oceanic shelf

Zooplankton was collected on the Newfoundland and Labrador shelf as part of the Atlantic Zone Monitoring Program (Therriault et al. 1998) from 21 July to 6 August 2003. Sampling of 45 stations located along five cross-shelf sections (Fig. 3a) was completed following the protocols outlined by Mitchell et al. (2002). The placement and length of the five transects ensures sampling across the major banks of the shelf and in the inner and outer branches of the Labrador Current. At each site, a zooplankton sample was collected using vertical tow of a 0.75-m net fitted with 0.202-mm nitex mesh, from a depth 5 m above the bottom, to a maximum depth of 1,000 m, to the surface. The tow speed was 1 m s^{-1}. Samples were preserved in a 4% solution of buffered formaldehyde. The analysis focused on the distribution of the copepod *C. finmarchicus*, a dominant species which plays a key role in the transfer of energy from phytoplankton to fish throughout much of the North Atlantic (Planque and Batten 2000). The abundance of *C. finmarchicus* was estimated from a subsample in which at least 150–200 specimens of all *Calanus* species (including two sister species, *C. glacialis* and *C. hyperboreus*) were counted and copepodites were staged. During the summer of 2003, *C. finmarchicus* represented from 30 to 100% (mean 74%) of the abundances of the three species.

In this region, the Labrador Current flows from north to south through an outer branch along the continental slope and an inner branch along the coast (Loder et al. 1998). There is some recirculation on the major banks, or topographic steering, so that turbulent eddy motion on the Newfoundland Shelf and the northern Grand Banks can be very important (Pepin and Helbig 1997). Major inflows of water carrying *C. finmarchicus* from the Labrador Sea take place through the cross-shelf channels located north and south of the three northernmost sections as well as across

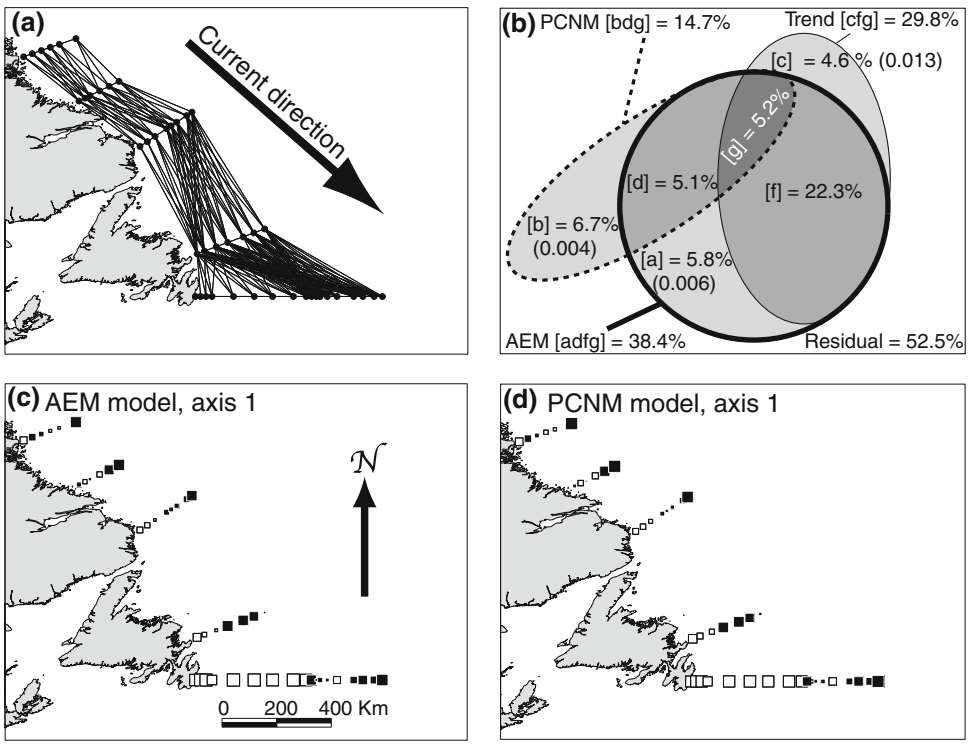

Fig. 3 Spatial modelling of *Calanus finmarchicus* distribution on oceanic shelf. **a** Site locations and connexion diagram used to generate the AEM eigenfunctions considering that current direction was used to generate AEMs. Square bubbles represent centred square-root transformed data (black are positive values, white are negative, size of squares is related to the associated value). Figure A3 (Appendix A) shows how all edges linking sites along a transect were used to build AEMs. **b** Variation partitioning results between the selected AEMs, PCNMs, and the trend are illustrated by a Venn diagram. Fraction sizes are approximations. Letters in brackets correspond to individual fractions of explained variation; values are R^2_a. Values in parentheses represent the P values of independent fractions. **c** First and only significant ($P < 0.001$) axis of a canonical RDA where the Hellinger transformed *C. finmarchicus* stages were explained by the selected AEM eigenfunctions; axis 1 accounts for 36.8% of the variation (black are positive values, white are negative, size of squares is related to the associated value). Axis 1 of the PCNM model is presented in the same way in (**d**); this axis represents 14.8% of the variation ($P = 0.005$)

the central Newfoundland Shelf at a latitude of approximately 50°N.

We analysed the abundances of the six copepodite stages of *C. finmarchicus* (the distribution of each stage is shown in Fig. D1, Appendix D). The analyses were done by RDA instead of multiple regression since the response data are multivariate. RDA is the multivariate extension of multiple linear regression (Legendre and Legendre 1998, Sect. 11.1). The analyses were performed following a Hellinger transformation of the multivariate *C. finmarchicus* data. After Hellinger transformation of frequency data (e.g., community composition), multivariate linear methods of analysis such as RDA preserve the Hellinger distance among the sites, which is appropriate for the analysis of community composition data, instead of the Euclidean distance which is inappropriate (Legendre and Gallagher 2001). Results of the three modelling methods revealed substantial differences in the modelled relationships among sites. Using AEM (f_3, $\beta = 2$), the set of positively autocorrelated variables explained 51.4% (R^2_a) of the variance. Forward selection retained AEM eigenfunctions #1 and 24 (Fig. D2, Appendix D), which yield an R^2_a of 38.4%. Detailed results for the other weighting functions considered are presented in Table D1 (Appendix D).

The full set of PCNMs variables explained 18.1% (R^2_a) of the detrended *C. finmarchicus* data. When forward selection was carried out, 2 PCNMs were selected (#2 and 11, presented in Fig. D3, Appendix D); they explained together 14.7% (R^2_a) of the non-detrended data. For MEM eigenfunctions applied to detrended data, no combination of f_3 and β was significant at the 5% level after Šidák correction; the best result ($\beta = 2$) was 16% of explained variation (R^2_a) with $P_{corr} = 0.195$. MEMs results will not be developed further owing to this last result.

Along and cross-shelf trends in the distribution of *C. finmarchicus* contributed greatly to the overall results, but the greater strength of the AEM model is clear (Fig. 3b). The values fitted to the AEM model along the first and only significant RDA axis, $P < 0.001$ (Fig. 3c), and the values fitted to the PCNM model along the first and only significant RDA axis, $P < 0.001$ (Fig. 3d), illustrate the cross-shelf gradient in the distributions of the *C. finmarchicus* copepodite stages, with offshore stations generally dominated by older stages while younger copepodites were more abundant close to the coast. Model results suggest that the cross-shelf distribution is set in the northernmost reaches of the region, with limited cross-shelf exchange. The dominant features of the AEM model are the general north-to-south pattern in association among stations along with the inshore-offshore separation in the southern portion of the region (Fig. 3c, d). There is some variability in the association among stations but the indication of mixing and recirculation across the northernmost sections and the gradual cross-shelf splitting of the inner and outer branches of the Labrador Current (and of the younger and older copepodite stages) in the middle and southern portions of the range is the only analysis that yields model results that are consistent with regional circulation on the Newfoundland Shelf. Drift simulations based on the climatological average seasonal circulation of Han et al. (2008) confirm that copepodites found on the continental shelf and Grand Banks along the southernmost transect come principally from sources located on the continental shelf in the northern part of the study area (P. Pepin and G. Han, unpublished data).

Understanding the source of *C. finmarchicus* on the inner shelf has important implications for interpreting observations from a site (S27: 47°32.5′N, 52°35.2′W) sampled twice a month that is used to monitor seasonal changes in population dynamics in the region. *C. finmarchicus* from sources near the northernmost area of the species range are subject to a shorter growing season than animals from the major population centre located in the southern Labrador Sea. This can limit their ability to accumulate energy reserves, in the form of wax esters, which will have implications for the individual's ability to enter diapause in the autumn and thereby affect the environment in which they will reproduce, and thus affect their potential fitness. Late stage copepodites (stage 5) of *C. finmarchicus* on the inner shelf have been shown to have smaller energy reserves (Pepin and Head 2009) and are more likely to moult into adults in the autumn than in the following spring relative to animals located in the Labrador Sea. This affects our understanding of seasonal patterns of secondary production in different parts of the region and has important implications for how production on the continental shelf may be affected by remote forcing from other parts of the North Atlantic subpolar gyre. This may also explain why inter-annual variations in abundance of *C. finmarchicus* on the inner shelf appear to be more similar to those in the northern portions of the study region relative to those in the southern Labrador Sea (Pepin et al. 2008; Pepin, unpublished data).

Discussion

The AEM framework shares the following property with the MEM framework: Moran's *I* values can be associated with the eigenfunctions representing the spatial relationships among sites. The main difference lies in the directional nature of the process represented by its eigenfunctions. The AEM framework constructs variables modelling directional (asymmetric) information whereas the MEM framework creates variables with evenly-weighted omnidirectional (symmetric) information. As shown in the examples

presented in this paper, the use of AEMs does not require the detrending of the response variables. There are two main reasons for this. Conceptually, AEMs are used when we can hypothesize that the process generating the response data is spatially directional and we want to estimate its influence on the response. Practically, the first AEM eigenfunction computed along a narrow river map, for example, is comparable to a half-sine wave, which models a broad-scale trend, whereas the first MEM eigenfunction is a full sine wave as shown in Borcard and Legendre (2002, Fig. 2). In Appendix E, we present an example where the sine waves of AEMs and MEMs are compared. This does not mean that the AEM framework should be used instead of the MEM framework when the general trend is significant. As seen in the bacterial production and *Atya* examples that did not contain significant trends, the choice of the framework to be used should be based on the hypothesis one wants to test about the physical processes at work in the system under study; AEM modelling is only used when a directional spatial process is hypothesized. Because PCNMs are a particular case of MEMs (Dray et al. 2006), they do not need to be discussed separately with regard to this point.

Calculation of different fractions, in variation partitioning, after modelling spatial distributions by non-directional (PCNM or MEM) and directional eigenfunctions (AEM), provided quantitative information about the directional and non-directional spatial processes taking place in the systems under study. The fractions of variation represented only by AEM (fraction [a] in all examples) can be interpreted as the directional influence of the spatial process on the data under study. The other fractions represent the non-directional spatial components.

We have shown with the help of the three ecological illustrations that the AEM framework can be used at any scale and that insights can be obtained at different scales within a particular system. The results in Figs. 1c, 2c, and 3c illustrate how different scales, at which the ecological processes studied occur within each system, are brought out by the analysis. In the *Atya* illustration (Fig. 1c), the selected AEM eigenfunctions differentiate the left and right sides of the river, with a wave length of roughly 25 m.

For the bacterial production illustration (Fig. 2c), the wave lengths within the three water masses are completely different. In the North portion of the lake, the spatial structure of the bacterial production has a wave length of roughly 7.5 km, whereas the South section is structured at wave lengths of over 20 km. The central water mass is even more broadly structured. In this water mass, it is likely that the spatial distribution of bacterial production is broader than the extent of the sampling area since AEM analysis cannot extract any spatial structure.

In the ocean example (Fig. 3c), the half-wave length within the transects broadens from North to South. In the northernmost transect, *C. finmarchicus* has a spatial half-wave length of about 75 km in the east–west direction. The middle transect uncovers a broader half-wave length of roughly 125 km in from east to west. The southernmost transect presents an even broader half-wave length of over 400 km.

The different wave lengths at which each system is structured can be the result of multiple factors (environmental, biological, anthropogenic, etc.) influencing directly or indirectly, independently or in combination, the organisms under study.

The examples presented in this paper have shown that the use of an appropriate method to model spatial relationships, such as the AEM framework for directional processes, may produce large R^2_a, providing a more complete understanding of the systems under study than less specific modelling methods. AEM eigenfunctions do not always explain all the variation that PCNMs and MEMs account for, but what is not explained by the set of asymmetric spatial variables is often small and not significant when the directional forcing process is strong. Even when the fraction related to the trend but not to the AEMs ([c] in Fig. 3b) is considered to belong to the symmetric methods, the amount of variation explained does not come close to what is explained by the AEM model independently. This is another point that favours the use of AEM modelling where there is a known asymmetric spatial structure possibly caused by a strong directional process.

The asymmetric eigenvector maps framework is a broad extension of the eigen-based spatial filtering method proposed by Griffith and Peres-Neto (2006), reinforcing this family of methods. It allows users to incorporate into the spatial model the knowledge they have about the spatial process they hypothesize to be influencing the response data. The choice of weights to be applied to the edges of the connexion diagram is as important in the AEM framework as it is in the MEM framework, a point stressed by Dray et al. (2006). However, the presence of the AEM framework in the eigen-based spatial filtering family of methods forces us to make a more general decision prior to that of weighting the edges: to choose the spatial context in which the studied data belong, directional or non-directional. This is an easy decision to take in the presence of strong spatial directional processes generating asymmetry, as found in the three examples in this paper. The same can be said when the response data is assumed to be symmetric. But what to do in situations where the system under study is known to be neither fully non-directional nor perfectly directional? A rudimentary answer has been given in this paper when constructing AEM for each example. Because there are edges perpendicular to the direction of the directional process, these had to be added in both directions; Fig. A3 (Appendix A) shows in detail how this

procedure was implemented. The use of both AEM and MEM variables, as was done in this paper, can help in better understanding situations that are not fully directional or non-directional.

The technical developments presented in Fig. A3 explain how co-occurring physical forcings can be dealt with. This approach helps deal with situations where physical forcing comes from different directions. For example, estuarine systems are known to be influenced by currents of different origins (e.g., ebb and flow currents). Using the approach presented in Fig. A3 with weights on the links that represent current velocity also makes AEM an asset for more complex systems than the examples presented in this paper.

Because this paper's aim was to compare different spatial modelling methods, symmetric and asymmetric, no environmental components were considered. The potential of combining AEMs and environmental variables in contexts where there is a known spatial asymmetry in the response data is interesting. To include non-spatial information in variation partitioning will produce a more complete and informative model and will result in a better understanding of the system under study.

Acknowledgements The work reported in this paper was supported by NSERC grant no. 7738-07 to P. Legendre. The work on Capesterre River was funded by grants from the Direction Régionale de l'Environnement de la Guadeloupe and the Parc National de la Guadeloupe to D. Monti. The work on Lake St-Pierre was funded by an NSERC Discovery and an FQRNT Strategic Professor grant to R. Maranger. The work off Newfoundland is the result of activities of the Atlantic Zone Monitoring Programme of Fisheries and Oceans Canada. The research conducted in this study is in compliance with the current laws of the country in which they were performed.

References

Blanchet FG, Legendre P, Borcard D (2008a) Forward selection of explanatory variables. Ecology 89:2623–2632

Blanchet FG, Legendre P, Borcard D (2008b) Modelling directional spatial processes in ecological data. Ecol Model 215:325–336

Blanchet C, Maltais-Landry G, Maranger R (in press) Variability in nitrogen content of submerged aquatic vegetation: utility as an indicator of N dynamics within and among lakes. Wat Sci Tech

Borcard D, Legendre P (2002) All-scale spatial analysis of ecological data by means of principal coordinates of neighbour matrices. Ecol Model 153:51–68

Borcard D, Legendre P, Drapeau P (1992) Partialling out the spatial component of ecological variation. Ecology 73:1045–1055

Borcard D, Legendre P, Avois-Jacquet C, Tuosimoto H (2004) Dissecting the spatial structure of ecological data at multiple scales. Ecology 85:1826–1832

Caraco NF, Lampman G, Cole JJ, Limburg KE, Pace ML, Fischer D (1998) Microbial assimilation of DIN in a nitrogen rich estuary: implications for food quality and isotope studies. Mar Ecol Progr Ser 167:59–71

Cole JJ, Caraco NF (2001) Carbon in catchments: connecting terrestrial carbon losses with aquatic metabolism. Mar Freshw Res 52:101–110

Cole JJ, Prairie YT, Caraco NF, McDowell WH, Tranvik LJ, Striegl RG, Duarte CM, Kortelainen P, Downing JA, Middelburg JJ, Melack J (2007) Plumbing the global carbon cycle: integrating inland waters into the terrestrial carbon budget. Ecosystems 10:172–185

Cressie N, Frey J, Harch B, Smith M (2006) Spatial prediction on a river network. J Agric Biol Environ Stat 11:127–150

del Giorgio PA, Pace ML (2008) Relative independence of dissolved organic carbon transport and processing in a large temperate river: the Hudson River as both pipe and reactor. Limnol Oceanogr 53:182–197

Dray S, Legendre P, Peres-Neto PR (2006) Spatial modelling: a comprehensive framework for principal coordinate analysis of neighbour matrices (PCNM). Ecol Modell 196:483–493

Ezekiel M (1930) Method of correlation analysis. Wiley, New York

Fortin MJ, Dale MRT (2005) Spatial analysis: a guide for ecologists. Cambridge University Press, Cambridge

Frenette JJ, Arts MT, Morin J, Gratton D, Martin C (2006) Hydrodynamic control of the underwater light climate in fluvial Lac Saint-Pierre. Limnol Oceanogr 51:2632–2645

Fryer G (1977) Studies on the functional morphology and ecology of the atyid prawns of Dominica. Philos Trans R Soc Lond B 277:57–129

Gittleman J, Kot M (1990) Adaptation: statistics and a null model for estimating phylogenetic effects. Syst Zool 39:227–241

Griffith DA, Peres-Neto PR (2006) Spatial modeling in ecology: the flexibility of eigenfunction spatial analyses. Ecology 87:2603–2613

Han G, Lu Z, Wang Z, Helbig J, Chen N, de Young B (2008) Seasonal variability of the Labrador Current and shelf circulation off Newfoundland. J Geophys Res 113:C10013. doi:10.1029/2007JC004376

Hopkinson CS, Giblin AE, Garrit RH, Tucker J, Hullar MAJ (1998) Influence of benthos on growth of planktonic estuarine bacteria. Aquat Microb Ecol 16:109–118

Hutchinson G (1957) Concluding remarks. Cold Spring Harbor Symp Quant Biol 22:415–427

Legendre P (1993) Spatial autocorrelation: trouble or new paradigm. Ecology 74:1659–1673

Legendre P, Fortin MJ (1989) Spatial pattern and ecological analysis. Vegetatio 80:107–138

Legendre P, Gallagher ED (2001) Ecologically meaningful transformations for ordination of species data. Oecologia 129:271–280

Legendre P, Legendre L (1998) Numerical ecology, 2nd English edn. Elsevier, Amsterdam, The Netherland

Loder JW, Petrie P, Gawarkiewicz G (1998) The coastal ocean off northeastern North America: a large scale view. In: Robinson AR, Brink KH (eds) The sea, Vol 11. Wiley, New York, pp 105–133

Maranger RJ, Pace ML, del Giorgio PA, Caraco NF, Cole JJ (2005) Longitudinal spatial patterns of bacterial production and respiration in a large River-Estuary: implications for ecosystems carbon consumption. Ecosystems 8:318–330

Masin M, Jezbera J, Nedoma J, Straskrabova V, Hejzlar J, Simek K (2003) Changes in bacterial community composition and microbial activities along the longitudinal axis of two canyon-shaped reservoirs with different inflow loading. Hydrobiologia 504:99–113

Mitchell MR, Harrison G, Pauley K, Gagné A, Maillet G, Strain P (2002) Atlantic zonal monitoring program sampling protocol. Can Tech Rep Hydrogr Ocean Sci 223: iv + 23

Newbold JD, O'Neill RV, Elwood JW, Van Winkle W (1982) Nutrient spiralling in streams: implications for nutrient limitation and invertebrate activity. Am Nat 120:628–652

Ohtani K (2000) Bootstrapping R^2 and adjusted R^2 in regression analysis. Econ Model 17:473–483

Pepin P, Head EJH (2009) Seasonal variation in the depth-dependent state of stage 5 copepodites of *Calanus finmarchicus* in the waters of the Newfoundland Shelf and the Labrador Sea. Deep-Sea Res (Part I) 56:989–1002

Pepin P, Helbig JA (1997) The distribution and drift of cod eggs and larvae on the Northeast Newfoundland Shelf. Can J Fish Aquat Sci 54:670–685

Pepin P, Maillet GL, Fraser S, Shears T, Redmond G (2008) Biological and chemical oceanographic conditions on the Newfoundland Shelf during 2007. CSAS Res Doc 2008/034, 61p

Peres-Neto PR, Legendre P, Dray S, Borcard D (2006) Variation partitioning of species data matrices: Estimation and comparison of fractions. Ecology 87:2614–2625

Peterson DL, Parker VT (1998) Ecological scale: theory and application. Columbia University Press, New York

Peterson EE, ver Hoef JM (2010) A mixed-model moving-average approach to geostatistical modeling in stream networks. Ecology 91:644–651

Peterson EE, Theobald DM, ver Hoef JM (2007) Geostatistical modelling on stream networks: developing valid covariance matrices based on hydrologic distance and stream flow. Freshw Biol 52:267–279

Planque B, Batten SD (2000) *Calanus finmarchicus* in the North Atlantic: the year of *Calanus* in the context of interdecadal change. ICES J Mar Sci 57:1528–1535

Pyron M, Covich AP, Black RW (1999) On the relative importance of pool morphology and woody debris to distributions of shrimp in a Puerto Rican headwater stream. Hydrobiologia 405:207–215

Rees GN, Beattie G, Bowen PM, Hart BT (2005) Heterotrophic bacterial production in the lower Murray River, south-eastern Australia. Mar Freshw Res 56:835–841

Šidák Z (1967) Rectangular confidence regions for the means of multivariate normal distributions. J Am Stat Assoc 62:626–633

Smith DC, Azam F (1992) A simple, economical method for measuring bacterial protein synthesis rates in seawater using ^{3}H-leucine. Mar Microb Food Webs 6:107–114

Therriault JC, Petrie B, Pepin P, Gagnon J, Gregory D, Helbig J, Herman A, Lefaivre D, Mitchell M, Pelchat B, Runge J, Sameoto D (1998) Proposal for a northwest Atlantic zonal monitoring program. Can Tech Rep Hydrogr Ocean Sci 194: vii + 57

ver Hoef JM, Peterson EE (2010) A moving average approach for spatial statistical models of stream networks. J Am Stat Assoc 105:6–18

ver Hoef JM, Peterson EE, Theobald DM (2006) Spatial statistical models that use flow and stream distance. Environ Ecol Stat 13:449–464

Vis C, Hudon C, Carignan R, Gagnon P (2007) Spatial analysis of production by macrophytes, phytoplankton and epiphyton in a large river system under different water-level conditions. Ecosystems 10:293–310

Wetzel RG (1992) Gradient-dominated ecosystems: sources and regulatory functions of dissolved organic matter in freshwater ecosystems. Hydrobiologia 229:181–198

Zar JH (1999) Biostatistical analysis, 4th edn. Prentice Hall, Upper Saddle River, NJ